

Effect of supercritical carbonation on the strength and heavy metal retention of cement-solidified fly ash

Xiaoxiong Zha^{a,*}, Jiaqian Ning^a, Mohamed Saafi^b, Lijun Dong^a, Jean-Baptiste Mawulé Dassekpo^a, Jianqiao Ye^{b,*}

^a Department of Civil and Environmental Engineering, Shenzhen Graduate School, Harbin Institute of Technology, 518055 China

^b Department of Engineering, Lancaster University, Lancaster LA1 4YR, UK

* Corresponding author.

E-mail address j.ye2@lancaster.ac.uk (J. Ye) and zhaxx@hit.edu.cn (X.X. Zha)

Abstract

This paper presents both experimental and multi-physics studies on the carbonation and heavy metal retention properties of cement-solidified fly ashes. Cement-solidified fly ash samples with 40% and 60% fly ash ratios were tested for carbonation depth after being supercritically carbonated. Tests were also carried out for compressive strength and retention capacity of heavy metals of the samples before and after supercritical carbonation. Using CO₂ absorption instead of calcium carbonate to measure carbonation degree, a multi-physics model was developed and combined with a leaching model to study the impact of carbonation on Cu and Pb leaching from the cement-solidified fly ash. The results show that supercritical carbonation has both positive and negative impacts on the strength and retention capability of heavy metals of the cement-solidified fly ashes, which suggests that both the carbonation conditions and the amount of fly ash recycled in cementitious materials should be properly controlled to maximize potential positive effect.

Keywords: Cement-solidified; supercritical carbonation; fly ash; compressive strength; leaching rate.

30

31 **1. Introduction**

32 Protection of the public from hazardous pollutants in the environment has always been an
33 important priority for most industrialized countries, where a significant portion of the pollutants
34 is related to the increasing demands for energy. The data published by the International Energy
35 Agency stated that the energy consumption had increased by 50.52% from 1990 to 2014.
36 Consequently, the appearance of environmental problems poses a serious threat to the living
37 environment of human beings, such as heavy metal pollution caused by municipal solid waste
38 incineration (MSWI) fly ash [1, 2], global warming due to carbon dioxide (CO₂) emissions [3],
39 and so forth.

40

41 Municipal solid waste (MSW) has been always one of the most challenging problems in the
42 management of modern cities. There are about 254 million tons of garbage produced annually
43 in China, namely approximately one kilogram per person per day, the total amount of which is
44 about one third of the world's annual trash output [4]. The rapid growth of waste causes serious
45 limitations in the development of a city, if it is not handled properly [5]Error! Reference
46 source not found.. In recent years, MSWI has been widely used owing to its advantage on
47 capacity reduction and energy recovery efficiency [6, 7]. However, the by-product of MSWI,
48 such as fly ash [8], contains heavy metals that still have serious negative impact on the
49 surrounding environment [9], or can even cause irreparable damage to human health. Therefore,
50 the environmental threat from fly ash cannot be ignored and the development of an economic,
51 efficient and eco-friendly application of fly ash is one of the most important measures to address
52 the current situation.

53

54 From the perspective of the construction industry, fly ash can be used as a cement replacement
55 material [10] to develop high performance concrete. Besides the superiority in the value of
56 recycling [11] and CO₂ emissions [12], fly ash can also reduce hydration heat and improve
57 workability [13], as well as durability of concrete [14]. A concrete component with a high fly
58 ash replacement ratio has little impact on the bond strength with conventional concrete [15],

59 which may also have higher shear strength [16]. Hence, using MSWI fly ash as partial
60 replacement for cement in concrete mixes is potentially feasible [17].

61
62 To further develop the potential material, the mechanical properties, durability and leaching
63 performance of the cement-solidified fly ash were studied [18, 19]. Cement solidification
64 technology is an effective waste solidification method, which obviously reduces the leaching
65 toxicity of harmful substances, especially heavy metals, in cement-solidified fly ash [17].
66 Leaching tests were also conducted to verify the feasibility of the technology [14]. Leaching in
67 a solidified body varies with water-cement ratios and also types of leachants, e.g. deionized or
68 mineralized water. Pure water appeared more aggressive than mineralized water [20]. Moreover,
69 a multi-physics leaching model of a solidified body was also developed and the simulation
70 results were compared with those from leaching experiment of Sr and Cs [21].

71
72 Cement-based materials are porous, in which the pores form the channels that leak heavy metals,
73 resulting in a reduced capacity of retaining them in the solidified body [22]. Carbonation of
74 cement-based materials can improve the pore structure of the material, and therefore reduces
75 its porosity [23]. The technique has been used to treat waste to reduce leaching toxicity of
76 certain metals [24]. Recently, research on accelerated and supercritical carbonation, i.e.,
77 carbonation under elevated temperature and pressure were carried out [21]. When the
78 temperature and pressure of CO₂ exceed their respective critical states ($T_c=31.26^\circ\text{C}$,
79 $P_c=7.39\text{MPa}$), the CO₂ is said under its supercritical state (SCC) [25]. Other supercritical
80 carbonation models of cement mortar and cement include Refs. [13, 26, 27]. To study the effect
81 of carbonation on the leaching resistance of hazardous waste cement solidification, Zha et al.
82 [21] develop a model using the finite element software COMSOL Multiphysics. The parametric
83 studies from the numerical simulations revealed that carbonation could significantly improve
84 the retention capability of cementitious solids containing hazardous wastes.

85
86 In this paper, further modifications on, e.g, the carbonation rate equation, specific heat of CO₂
87 and change of porosity caused by carbonation, are made based on the simulation model

88 proposed by Zha et al. [27] for cement-solidified fly ash. The simplified form of the leaching
 89 model [21] is adopted to estimate the leaching of Cu and Pb. The carbonation and leaching
 90 models are used together to build a combined model for the multi-physics carbonation-leaching
 91 problem. Then, carbonation, strength and leaching experiments are carried out for 40% and 60%
 92 cement-solidified fly ash to validate the modified models and study the effect of carbonation
 93 and fly ash ratio on the performance of the cement-solidified fly ash.

94

95 **2. Mathematical modeling**

96 **2.1 Equations of supercritical carbonation process**

97 Based on the natural carbonation model by Saetta et al. [23], Zha et al. [27] proposed a model
 98 for supercritical carbonation, where (1) Darcy's law was used in place of Fick's law; and (2)
 99 the change of CO₂ concentration in pore solution was assumed to be equal to that of its solubility,
 100 i.e., assuming that there was always sufficient dissolved CO₂ to participate in the carbonation
 101 reaction under supercritical carbonation conditions.

102

103 The equations to be solved include the carbonation rate equation, the mass conservation
 104 equation of CO₂, the gas-liquid two-phase flow equations and the energy conservation equation,
 105 as shown in equation (1).

$$\left\{ \begin{array}{l} \frac{\partial R_c}{\partial t} = \alpha_1 f_1(h) f_2(g) f_3(R_c) f_4(T) \\ \frac{\partial g}{\partial t} = \frac{\partial m_c}{\partial t} \\ \frac{\partial (n S_\alpha \rho_\alpha)}{\partial t} + \nabla \cdot (\rho_\alpha \mathbf{v}_\alpha) = q_\alpha \\ \mathbf{v}_\alpha = - \frac{k \cdot k_{ra}}{\mu_\alpha} (\Delta P_\alpha) \\ (\rho C_q)_{eff} \frac{\partial T}{\partial t} = \nabla \cdot (k_{eff} \nabla T) - (C_g \rho_g \mathbf{u} \mathbf{v}_g + C_w \rho_w \mathbf{u} \mathbf{v}_w) \cdot \nabla T \end{array} \right. \quad (1)$$

106 where R_c is the degree of carbonation; α_1 is the carbonation rate coefficient, indicating the
 107 variation rate of carbonation degree under ideal conditions; $f_1(h)$, $f_2(g)$, $f_3(R_c)$ and $f_4(T)$ denote,
 108 respectively, the effect of humidity, CO₂ concentration, carbonation degree and temperature on
 109 the carbonation rate; g is the mass concentration of CO₂; m_c is the solubility; n is the porosity

110 of the cement-based materials; S_α , ρ_α , μ_α^v , q_α , k_{ra} , μ_α , P_α and C_α are the saturation, density, Darcy
 111 velocity, source term accounting for chemical reaction or precipitation, relative permeability
 112 coefficient, dynamic viscosity, pressure and specific heat of component α , respectively. The
 113 subscript, α , can be either g or w denoting gas or liquid phases, respectively; k is the inherent
 114 permeability; $(\rho C_q)_{eff}$ is the equivalent heat capacity; k_{eff} is the equivalent thermal conductivity.

115 **2.2 Modification of carbonation equations**

116 Numerous studies on supercritical carbonation of cement-based materials have been conducted
 117 [27-29]. However, the adopted theory, e.g., equation (1), is not generally applicable to all the
 118 cement-based materials, especially to the materials with admixtures. In this paper, some
 119 modifications are introduced to extend its applicability to include cement-solidified fly ash.

120 **2.2.1 Modified carbonation reaction rate equation**

121 The main chemical reactions during the carbonation process of cement-based materials are
 122 shown in equation (2), in which C-S-H stands for calcium silicate hydrate.



123 The carbonation rate was estimated in the previous model [27] on the basis of the measurement
 124 of the calcium carbonates generated during the process, i.e., the carbonation degree is calculated
 125 by the following equation:

$$R_c = \frac{cc}{cc_{max}} \quad (3)$$

126 where cc is the amount of calcium carbonate produced in the carbonation process and cc_{max} is
 127 the cc when the material is fully carbonated.

128
 129 However, the using of calcium carbonate production to measure carbonation degree has its
 130 limitations and can be inaccurate in assessing carbonation degree. Calcium carbonate generated
 131 by carbonation is an insoluble substance which can be trace dissolved in the pore solution, and
 132 reacts with CO_2 and water to form dissolvable calcium bicarbonate under high levels of
 133 dissolved CO_2 [30]. Also, calcium carbonate exists not only with the form of the single-

134 compound in carbonated cement-based materials, but also binds to other remaining products,
 135 e.g. to SiO₂ and H₂O to form xCaCO₃·ySiO₂·zH₂O [31]. This paper proposed an alternative
 136 estimation of carbonation degree based on measuring the CO₂ absorbed in the carbonation
 137 process, which takes a full account of all reactions with CO₂. Hence the following carbonation
 138 degree equation is proposed:

$$R_c = \frac{c}{c_{max}} \quad (4)$$

139 where c is the CO₂ absorbed by cement-based materials, c_{max} is the CO₂ absorbed after being
 140 fully carbonated, which can be assessed by phenolphthalein indicator [32] that changes the
 141 color of any non-carbonated cement to pink. The indicator is a 1% phenolphthalein ethanol
 142 solution with 1g phenolphthalein and 95% ethanol diluted to 100 ml. The calculation method
 143 of c_{max} will be discussed in the next section.

144 Introducing equation (4) into the first equation of equation (1) yields,
 145

$$\frac{\partial c}{\partial t} = \alpha_1 f_1(h) f_2(g) f_3(c) f_4(T) \quad (5)$$

146 where $f_3(c)$ denotes the effect of the absorbed CO₂ on the carbonation rate, which is calculated
 147 by.

$$f_3(c) = c_{max} - c \quad (6)$$

148 **2.2.2 Determination of c_{max}**

149 The calculation of the maximum CO₂ absorbed per unit volume by cement-based materials in
 150 the ideal state is proposed below, which is related to the amount of calcium, iron, and aluminum
 151 oxides in the material [33].

$$c_{max} = m_0 \left(\frac{[CaO]}{M_{CaO}} - 4 \frac{[Fe_2O_3]}{M_{Fe_2O_3}} - 4 \frac{[Al_2O_3]}{M_{Al_2O_3}} \right) \quad (7)$$

152 where, m_0 , in kg/m³, is the amount of cement per cubic meter cement-based materials; M and
 153 $[*]$, in which * can be CaO, Fe₂O₃ or Al₂O₃, represent the molar mass and the mole fraction of
 154 metallic oxide in cement, respectively. In equation (7), $M_{CaO} = 0.056$ kg/mol, $M_{Fe_2O_3} = 0.16$

155 kg/mol and $M_{Al_2O_3} = 0.102$ kg/mol.

156

157 Because the dimension of c_{max} is $\text{mol}\cdot\text{m}^{-3}$ in equation (7) and $\text{kg}\cdot\text{m}^{-3}$ in equation (6), Equation

158 (7) is modified as follows:

$$c_{\max} = M_c m_0 \left(\frac{[CaO]}{M_{CaO}} - 4 \frac{[Fe_2O_3]}{M_{Fe_2O_3}} - 4 \frac{[Al_2O_3]}{M_{Al_2O_3}} \right) \quad (8a)$$

159 where M_c is the molar mass of CO_2 ($M_c = 0.044$ kg/mol).

160

161 When cement is partially replaced with admixtures that have similar chemical components, (e.g.

162 fly ash with major chemical constituents CaO , SiO_2 , Al_2O_3 and Fe_2O_3), the hydration and

163 carbonation of the resulting admixtures should be considered. However, the chemical

164 composition of fly ashes depends on the characteristics and composition of the coal burned in

165 e.g., a power station. Berry [22] demonstrated that there was a wide range of fly ash

166 compositions. Fly ash is generally classified as Low-calcium Fly Ash (LFA, $<10\%$ CaO) and

167 High-calcium Fly Ash (HFA, $\geq 10\%$ CaO). For LFA, the c_{max} calculated by equation (8a) using

168 the fly ash compositions in Refs. [34, 35] is negative, and for HFA, the c_{max} calculated using the

169 fly ash compositions in Ref. [36] is ignorable when compared to that calculated for Ordinary

170 Portland Cement (OPC) [37]. Thus, in this paper, the contribution of fly ash to CO_2 absorption

171 of the cement-solidified is ignored.

172

173 Additionally, the amount of CO_2 absorbed during the carbonation process can be significantly

174 reduced due to the following two reasons: (1) cement-based materials are porous material

175 having large quantity of small and closed pores, which makes it difficult for the internal

176 materials to contact with CO_2 ; and (2) the precipitations generated in the carbonation process

177 accumulate on the inner surface of pores and clog the transport channels of CO_2 , and then

178 prevent the reaction from proceeding. Thus, equation (8a) can be modified by introducing a

179 reduction factor, α , as shown in equation (8b) below.

$$c_{\max} = \alpha M_c m_0 \left(\frac{[CaO]}{M_{CaO}} - 4 \frac{[Fe_2O_3]}{M_{Fe_2O_3}} - 4 \frac{[Al_2O_3]}{M_{Al_2O_3}} \right) \quad (8b)$$

180

181 This paper combines numerical and experimental methods to estimate the reduction factor α ,
182 as follows.

183 The CO₂ absorbed by a micro-volume of cement sample can be expressed as:

$$dm = R_c c_{\max} dv \quad (9)$$

184 where dm is the weight increment of dv after carbonation. Hence, m can be obtained by
185 integrating equation (9) over the whole cement sample.

$$m = \iiint_V R_c c_{\max} dv = c_{\max} \iiint_V R_c dv \quad (10)$$

186 where m is the weight increase of cement sample after carbonation. The cylindrical Ordinary
187 Portland Cement (OPC) paste samples having the same diameter and height of 50mm were
188 used for carbonation. The chemical components of the OPC are CaO, Fe₂O₃ and Al₂O₃ with
189 weights of 61.87%, 5.26% and 5.14%, respectively [37]. The average weight increase measured
190 after carbonation was about 4.21g. A numerical model was developed and calibrated against

191 the experimental c_{\max} , and $\iiint_V R_c dv$ was calculated by volume integration using COMSOL.

192 By combining the experiment and simulation results, the reduction factor calculated by
193 equations (10) and (8b) was $\alpha=0.178$, which, in principal, is affected by multi-factors, such
194 as composition, mixing rule, pore characteristics, etc. Because of the limitation of the
195 experiments, 0.178 was used in the simulations (section 3) as the reduction factor for all the
196 CCFC composites and verified against the experimental results (section 4). Clearly, further
197 studies on the relationship between the reduction factor and the influential factors are needed,
198 which requires additional extensive experimental work.

199

200 **2.2.3 Modification on the CO₂ specific heat**

201 The specific heat of CO₂ at constant pressure was adopted previously in the equation (1).

202 However, the pressure may change in a carbonation process, due to, e.g. a gradual reduction of
203 available CO₂ as carbonation is progressing. Naturally, the effect of pressure on the specific
204 heat of CO₂ should be considered. Researches on specific heat of CO₂ for different temperature

205 and pressure have been conducted by Li et al. [38] and Shi et al. [39]. The specific heat for 35°C
 206 and a pressure of 7.0 to 8.0MPa, which was proposed by Shi et al. [39], is used here for the
 207 supercritical condition, as follows:

$$C_c = \frac{40 + 11.5 \times (P_c - 7)}{M_c} \quad (11)$$

208 where P_c , M_c are the pressure and molar mass of CO_2 , respectively.

209 **2.2.4 Modification on the change of porosity**

210 The change in porosity is the key factor for its close link to the leaching behavior of the
 211 solidified cement. The following equation [40] was adopted previously in Zha et al. [27]:

$$n = \begin{cases} n_0(1 - 0.5R_c) & 0 \leq R_c \leq 0.4 \\ 0.8 \cdot n_0 & 0.4 \leq R_c \leq 1 \end{cases} \quad (12)$$

212 where n_0 is the porosity of the cement-based materials before carbonation.

213 Equation (12) only considers the effect of $\text{Ca}(\text{OH})_2$ on porosity and ignores the effect of other
 214 materials in the cement-based materials, such as C-S-H, un-hydrated $2\text{CaO} \cdot \text{SiO}_2$ and
 215 $3\text{CaO} \cdot \text{SiO}_2$. Shen et al. [26] reported that the porosity of cement-based materials after
 216 carbonation could be reduced by more than 50%, which was larger than the value calculated by
 217 equation (12). Other literatures [21, 26, 41] also mentioned that porosity reduction could reach
 218 up to above 70%. Hence, a mathematical model based on the experiment results of Zha et al.
 219 [21], which is more accurate to reflect the variation of porosity during carbonation, is proposed
 220 below:
 221

$$n = \begin{cases} 0.4n_0 & 0.9 < R_c \leq 1 \\ (0.85 - 0.5R_c)n_0 & 0.5 \leq R_c \leq 0.9 \\ (1 - 0.8R_c)n_0 & 0 \leq R_c < 0.5 \end{cases} \quad (13)$$

222 **2.3 Equation of leaching process**

223 Zha et al. [21] established the partial differential equations of leaching process on the base of
 224 Song et al. [42], which was according to the theory of non-equilibrium thermodynamic.
 225 However, from GB/T 7023-2011 [43] for leaching tests, temperature is required to be constant
 226 during the leaching process. The effect of temperature on the leaching is, therefore, neglected

227 in this paper, resulting in the following equation:

$$\nabla \cdot [\rho D \nabla C] - \lambda' \rho C + F = \rho \frac{\partial C}{\partial t} \quad (14)$$

228 where ρ is the density of the cement-based materials; D is the effective coefficient of diffusion;
229 λ' is the decay constant; F denotes the constant of absorption rate; C is the mass concentration
230 of the leaching elements, which varies with position and time, i.e., $C = f(x, y, z, t)$.

231 **2.4 Calculation of chemical activity factor**

232 The chemical activity factor was introduced to consider the effect of chemical fixation on the
233 diffusion coefficient in Zha et al. [21], and it was expressed by the ratio of free element
234 concentration to the total element. The respective values adopted for Sr and Cs was 0.7 and
235 0.06 [21]. Obviously, there is great difference in chemical activity factor for different elements,
236 which might depend on the pH and the chemical compositions in a cement-solidified material.

237
238 However, to the authors' best knowledge, there is no published researches on the calculation of
239 chemical activity factor during a carbonation process. In this paper, the chemical activity factors
240 of Pb and Cu were evaluated backwardly from the leaching experiment results against
241 carbonation degree. The obtained chemical activity factors of Pb and Cu are, respectively,

$$r_1 = (1 - 0.8R_c^2) \cdot r_{01} \quad (15)$$

$$r_2 = (1 + 33R_c) \cdot r_{02} \quad (16)$$

242 where r_1 , r_2 are the chemical activity factors of Pb and Cu respectively during carbonation,
243 while r_{01} and r_{02} are their initial values.

244

245 **3. Numerical simulation**

246 **3.1 Geometric model**

247 In this section, carbonation and leaching of cement-solidified fly ash are simulated using the
248 finite element software COMSOL. The solidified cement block is cylindrical having the same
249 diameter and height of 50mm, which is placed within a cylindrical container of 120mm in
250 diameter and 115mm in height, as shown in Fig. 1.

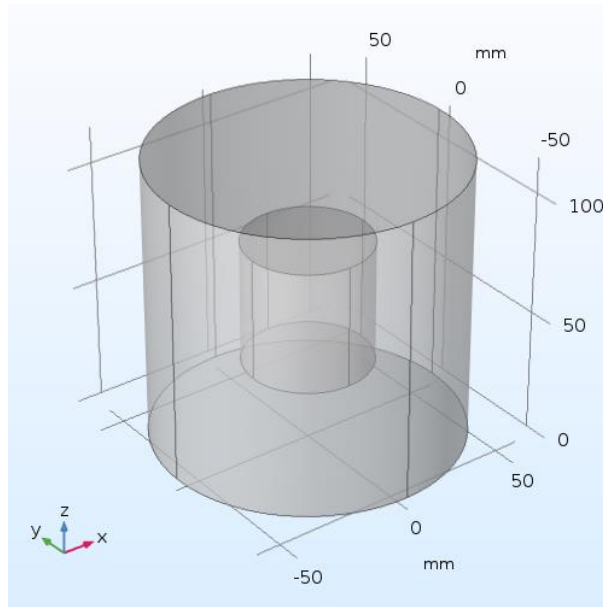
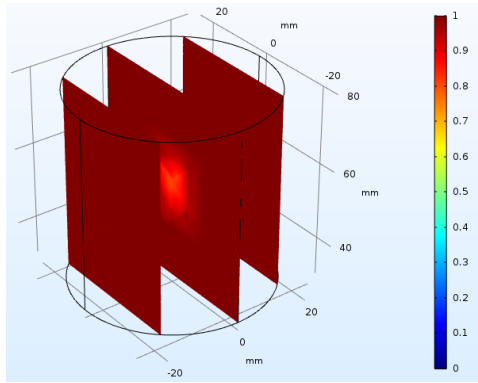


Fig. 1 Geometry of carbonation and leaching model

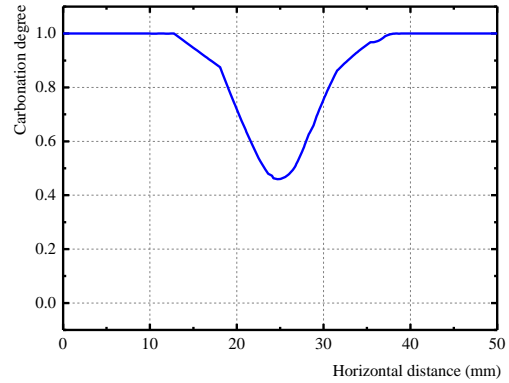
3.2 Carbonation model

The carbonation process using the modified model in Section 2.2 is simulated by COMSOL with specified initial values of $R_c=0$, $P_g=1atm$, $P_w=P_w0$, $T=T_0$ and $g=0$. Furthermore, the boundary conditions are modeled to represent, as close as possible, the actual reaction conditions in the laboratory experiments. As to the carbonation degree R_c and the CO_2 concentration g , both mathematically satisfied the Neumann boundary conditions, i.e., $\vec{n} \cdot \nabla R_c = 0$, and $\vec{n} \cdot \nabla g = 0$, respectively. The pressure and temperature used in the carbonation model were obtained from those measured in the experiments

The carbonation process is closely related to the chemical compositions in the cement-based materials. c_{max} was introduced previously in the paper to distinguish the content of CO_2 absorbed by different cement-based materials after full carbonation, and the cement-solidified samples with 40% and 60% fly ash were chosen to validate the modified model. The respective c_{max} calculated from equation (8b) are 46.6 kg/m^3 and 34.1 kg/m^3 . After carbonated for 3 hours, the carbonation degree (R_c) obtained by Zha et al. [27] and the current model on the vertical sections across the center are shown in Fig. 2 and Fig. 3, respectively.

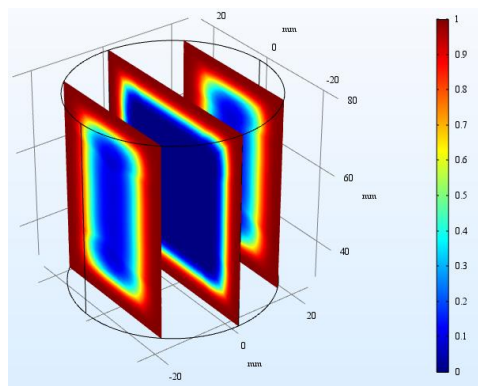


(a) R_c on sections-(40%, 60%)

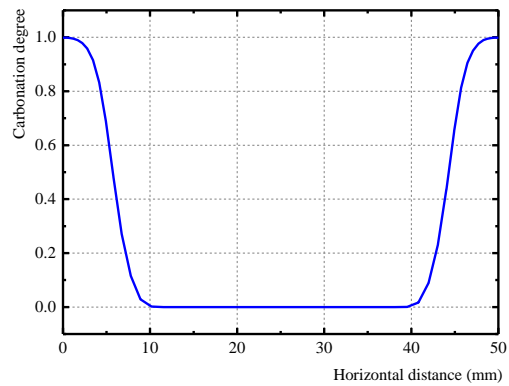


(b) R_c on transversal-(40%, 60%)

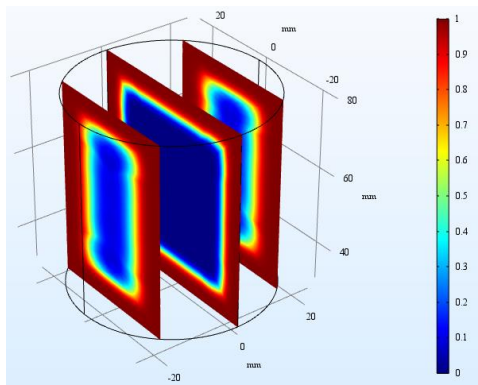
Fig. 2 Simulation results based on Zha et al. [27]



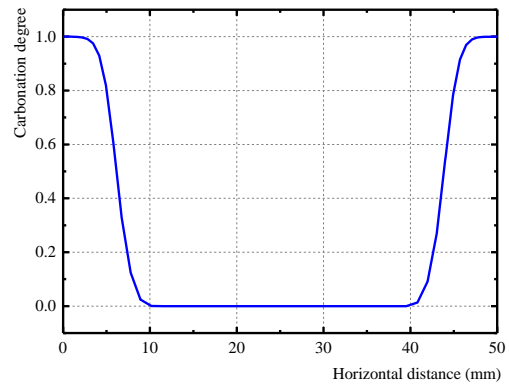
(a) R_c on sections-(40%)



(b) R_c on transversal-(40%)



(c) R_c on sections-(60%)



(d) R_c on transversal-(60%)

Fig. 3 Simulation results based on the modified model

269
270

By using the model proposed in Zha et al. [27], it is not possible to consider the variation of fly

271

ash ratio in the calculation of carbonation degree, as shown in Fig. 2, while it can be taken into

272

account now by the modified model, as shown in Fig. 3. This is due to the introduction of C_{max}

273

that is different for different fly ash ratios (equation (8b)). In the simulation, a region is judged

274 as fully carbonated when its R_c is larger than 0.99. The carbonation depth from Fig. 2 is about
275 12mm, and those obtained from Fig. 3 are about 2.3mm and 3.5mm, respectively, for cement-
276 solidified units with 40% and 60% fly ash. The experiment studies of these will be shown in
277 Section 4.2.

278 3.3 Leaching model

279 In the leaching process, the initial ion concentration C in the leachant and the cement-solidified
280 samples are set as $C=0$, $C=C_0$, respectively. The leaching from the samples to the leachant are
281 assumed to be diffusion and due to concentration difference. The boundary of the leaching
282 container is set as an insulation boundary, which is expressed by the Neumann boundary
283 condition, $\vec{n} \cdot \nabla C = 0$.

284 3.4 Combined model

285 The independent carbonation and leaching models developed from the above sections are
286 combined to form a continuous modeling process by introducing the carbonation results, e.g.
287 the reduced porosity caused by carbonation, directly into the leaching model. It is worth noting
288 that the diffusion coefficient of the leaching process should be set to zero at the carbonation
289 process to prevent any leaching, while the carbonation rate coefficient is set to zero during the
290 leaching process.

291

292 4. Experiments

293 4.1 Sample preparation

294 The main materials used in this study are Ordinary Portland Cement (OPC) and Fly Ash (FA).
295 The fly ash was supplied from Nanshan waste incineration power plant in Shenzhen. To avoid
296 the extreme situations, i.e. the strength of the sample is too low [44, 45] or the leaching
297 concentration of heavy metals is too small to measure, 40% and 60% fly ash ratios in cement-
298 solidified were investigated in this study. The mixture design of the samples is presented in
299 Table 1. Each of the samples was cast into a cylinder having the same diameter and height of
300 50mm.

301

302

Table 1 The mixture of the cement-solidified fly ash samples

Mass ratio of fly ash	Components	Mass (g)	Mixing time(min)	Sample No.
40%	Cement	1500	15	2/3-1~2/3-19
	Fly ash	1000		
	Water	1400		
60%	Cement	1000	15	3/2-1~3/2-19
	Fly ash	1500		
	Water	1400		

303

304 The average initial Cu and Pb contents of the cement-solidified fly ash samples are shown in

305 [Table 2](#), which were used also in the simulations (Section 3.3) to calculate the leaching rate.

306

Table 2 Cu and Pb contents in a sample

Element	40% fly ash sample (g)	60% fly ash sample (g)
Cu	0.0309	0.0452
Pb	0.1006	0.1462

307

308 **4.2 Carbonation**

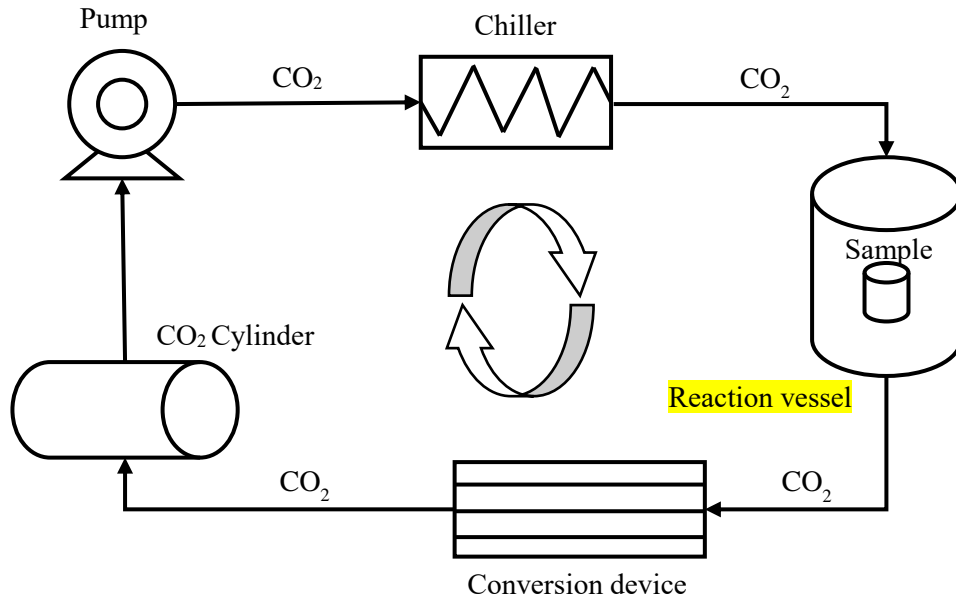
309 After being cured for 28 days, the cement-solidified fly ash samples were carbonated using the

310 CO₂ closed-cycle test system including the high-temperature and high-pressure reaction vessel,311 as shown in [Fig. 4 \[21\]](#). The closed-cycle system was designed to recycle the CO₂ and minimize312 the amount of CO₂ entering the atmosphere. In the process of carbonation, the temperature was

313 primarily controlled by the chiller, and the pressure was controlled by the pump. The controlled

314 pressure and temperature curves are shown in [Fig. 5](#). It is worth noting that the carbonation

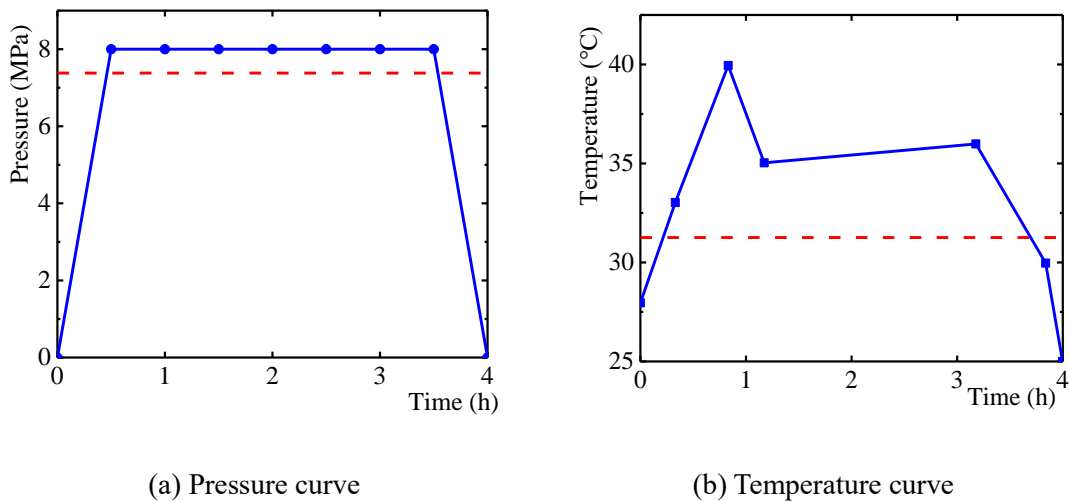
315 simulations were run only for the duration when the pressure is stabilized.



316

317

Fig. 4 CO₂ closed-cycle test system [21]



(a) Pressure curve

(b) Temperature curve

Fig. 5 Supercritical carbonation conditions

318

319 In order to determine whether the cement-solidified samples were carbonated, the mass of the

320 cement-solidified fly ash before and after carbonation were measured and is shown in Table 3.

321 The results show that the average percentages of mass increases of the samples are 5.416 (40%

322 fly ash) and 4.288 (60% fly ash), respectively. The mass increases of the samples with 40%

323 fly ash are generally larger than those of 60% fly ash, which is attributed to the larger amount of

324 mineral components (alkaline components) in the 40% than the 60% fly ash samples. The 40%

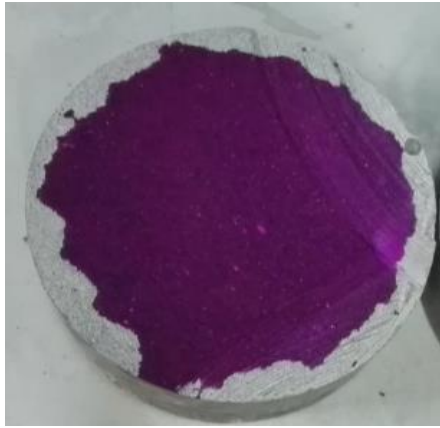
325 fly ash samples absorbed more CO₂, i.e. gained more weight than those of the 60% fly ash to

326 reach the same carbonation degree, which is also demonstrated by the calculation of c_{max} that
 327 are 46.6 kg/m³ and 34.1 kg/m³, respectively for the 40% and 60% cement-solidified fly ash.

328 Table 3 Mass increase percentages of the cement-solidified samples after carbonation

Mass ratio of fly ash	Sample No	Mass before carbonation (g)	Mass after carbonation (g)	Mass increase percentage (%)	Average mass increase percentage (%)
40%	2/3-1	167.9	177.7	5.837	5.146
	2/3-4	170.6	179.7	5.334	
	2/3-6	172.5	180.5	4.638	
	2/3-10	173.3	181.8	4.905	
	2/3-11	164.5	171.7	4.377	
	2/3-14	164.5	174.0	5.775	
	2/3-16	169.5	176.4	4.071	
	2/3-19	168.5	176.4	4.071	
60%	3/2-6	164.0	170.8	4.146	4.288
	3/2-7	163.9	172.0	4.942	
	3/2-8	167.3	174.3	4.184	
	3/2-11	171.5	176.0	2.624	
	3/2-14	163.4	172.4	5.508	
	3/2-15	165.4	171.4	3.628	
	3/2-18	164.2	170.8	4.019	
	3/2-19	163.6	172.2	5.257	

329
 330 In order to measure carbonation depth, the cross sections of the 40% and 60% fly ash samples
 331 were, respectively, inspected. Phenolphthalein indicator was sprayed on the cut and the un-
 332 carbonated zones changed color, as shown in Fig. 6. It is evident from the color change that
 333 cement-solidified fly ash samples were carbonated as the CO₂ penetration from the outside
 334 surfaces.



(a) 40% fly ash



(b) 60% fly ash

Fig. 6 Carbonation depth of the cement-solidified fly ash samples

335
336 Carbonation depths were measured at 88 points randomly selected along the carbonation front
337 of each samples. The average depths of the 40% and 60% fly ash sample are, respectively
338 2.1mm and 3.0mm. The test results agree well with the simulation carbonation depths based on
339 the modified model (respectively, 2.3mm and 3.5mm), but are significantly different with those
340 based on Zha et al. [27] (about 12mm). The results show that the capability of absorbing CO₂
341 varies with chemical compositions, which further influences carbonation depth. The above
342 comparisons confirm that using CO₂ absorption, c , rather than calcium carbonate production to
343 measure carbonation degree in simulations is more accurate.

344 **4.3 Strength test**

345 Strength tests were also carried out on the samples before and after carbonation. The cement-
346 solidified fly ash samples were divided into 4 groups in the test, i.e. the 40% cement-solidified
347 fly ash before and after carbonation; the 60% cement-solidified fly ash before and after
348 carbonation. Each un-carbonated group had 5 samples, while each carbonated group had 3
349 samples that had been carbonated for 3 hours under the supercritical condition. The test results
350 are listed in [Table 4](#).

351 Table 4 Strength of the samples

Group	Sample No	Strength (MPa)	Average strength (MPa)
Non-carbonated 40% fly ash	2/3-12	23.4	20.9
	2/3-13	17.1	
	2/3-15	20.2	
	2/3-17	20.6	
	2/3-18	23.5	
Carbonated 40% fly ash	2/3-4	17.9	17.1
	2/3-6	16.7	
	2/3-14	16.7	
Non-carbonated 60% fly ash	3/2-3	9.1	9.1
	3/2-7	7.1	
	3/2-9	10.4	
	3/2-10	9.2	
	3/2-16	9.6	
Carbonated 60% fly ash	3/2-6	7.2	7.6
	3/2-11	7.8	
	3/2-19	7.8	

352

353 It is apparent from the test results that the overall strength of the carbonated samples is lower
354 than that of the samples before carbonation. This is different from Li [28] on cement blocks
355 without added fly ash, where the strength of cement block increased by more than 60% after
356 carbonation. For the cement blocks tested here, the replacement of cement by fly ash reduced
357 the size of pores [46], which made the block more sensitive to micro cracks due to the expansion
358 of pores caused by the calcium carbonate produced during carbonation process. The earlier
359 formation of the micro-cracks contributed to the reduction in strength of the cement-solidified
360 fly ash.

361

362 However, the results agree with Junior et al. [47], where the compressive strength of cement
363 paste decreased after being carbonated for 4 hours, though increase in strength occurred during
364 the first 1-2 hours carbonation. Junior et al. [47] also showed that the longer the carbonation
365 duration was (more than 4 hours), the greater the strength reduction would be. These might
366 attribute to the fact that the generated calcium carbonate had exceeded the limit of the pores,

367 which caused additional internal pressure and micro-crack [30]. In this paper, the cement-
 368 solidified fly ash was subject to supercritical carbonation, resulting to a quick accumulation of
 369 calcium carbonate in the pores and an earlier reduction in strength.

370
 371 Table 4 also shows that the average strength of the 40% samples is more than twice that of the
 372 60% samples for before and after carbonation, i.e., the strength of the cement-solidified samples
 373 is greatly reduced as the content of fly ash increases. The results agree with those of Lombardi
 374 et al. [48], which showed that the amount of strength reduction with fly ash/cement ratio varying
 375 from 0.75 to 1.5 was about 50% which is in line with the reduction (56.5% for un-carbonated
 376 samples, 55.6% for carbonated samples) observed from this study. In summary, the duration of
 377 carbonation and the proportion of fly ash added in cement-solidified fly ash should be properly
 378 administrated to optimize their recycling value.

379

380 **4.4 Leaching experiment**

381 *4.4.1 Experiment equipment and process*

382 The cement-solidified fly ash samples required simple surface treatment to remove stains before
 383 the leaching experiment. They were placed in pre-cleaned leaching containers. 1.2 L deionized
 384 water was injected into each of the containers to submerge the samples. The containers were
 385 then sealed and placed in a leaching chamber of constant temperature ready for the leaching
 386 experiment.

387

388 Twenty cement-solidified fly ash samples were tested in the leaching experiment, which were
 389 divided into 4 groups as shown in Table 5. Each of the groups have 5 samples with the same
 390 fly ash ratio and carbonation time. The total leaching time is 42 days. Leaching rates at days 1,
 391 3, 7, 10, 14, 21, 28, 35 and 42 were measured and group averages were calculated.

392

Table 5 Details of leaching experiment

Group	Sample No	Leaching temperature($^{\circ}$ C)
Non-carbonated 40% fly ash	2/3-2,2/3-3,2/3-7,2/3-8,2/3-9	25

Group	Sample No	Leaching temperature(°C)
Carbonated 40% fly ash	2/3-1,2/3-10,2/3-11,2/3-16,2/3-19	
Non-carbonated 60% fly ash	3/2-1,3/2-2,3/2-4,3/2-5,3/2-12	
Carbonated 40% fly ash	3/2-7,3/2-8,3/2-14,3/2-15,3/2-18	

393

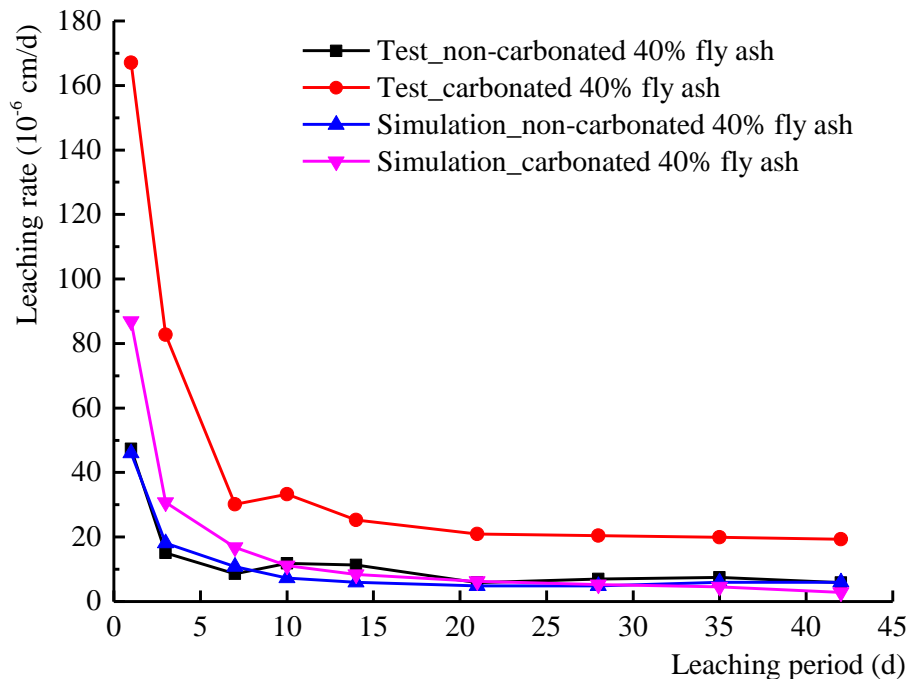
394 The method recommended by GB/T 7023-2011 [43] was used to calculate the leaching rate of
 395 the cement-solidified fly ash.

$$R_n = \frac{a_n / A_0}{(S / V)(\Delta t)_n} \quad (17)$$

396 where R_n is the leaching rate of heavy metals in the n^{th} leaching period (cm/d), a_n is the leaching
 397 mass in the n^{th} leaching period (g), A_0 is the initial mass of heavy metals in the cement-solidified
 398 fly ash (g), S is the contact area of the sample and leachant (cm^2), V is the volume of sample,
 399 and $(\Delta t)_n$ is the days of the n^{th} leaching period (d).

400 4.4.2 Results and analysis

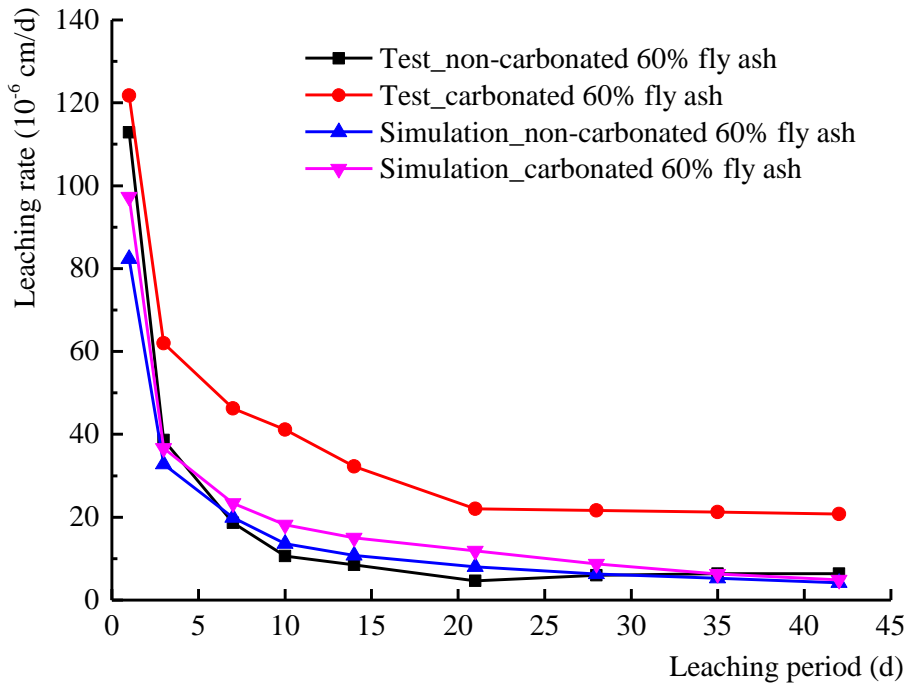
401 The leaching rates of Cu in the 40% and the 60% cement-solidified fly ash are shown,
 402 respectively, in Figs. 7 and 8, and those of Pb in the 40% and the 60% cement-solidified fly ash
 403 are shown, respectively, in Figs. 9 and 10.



404

405

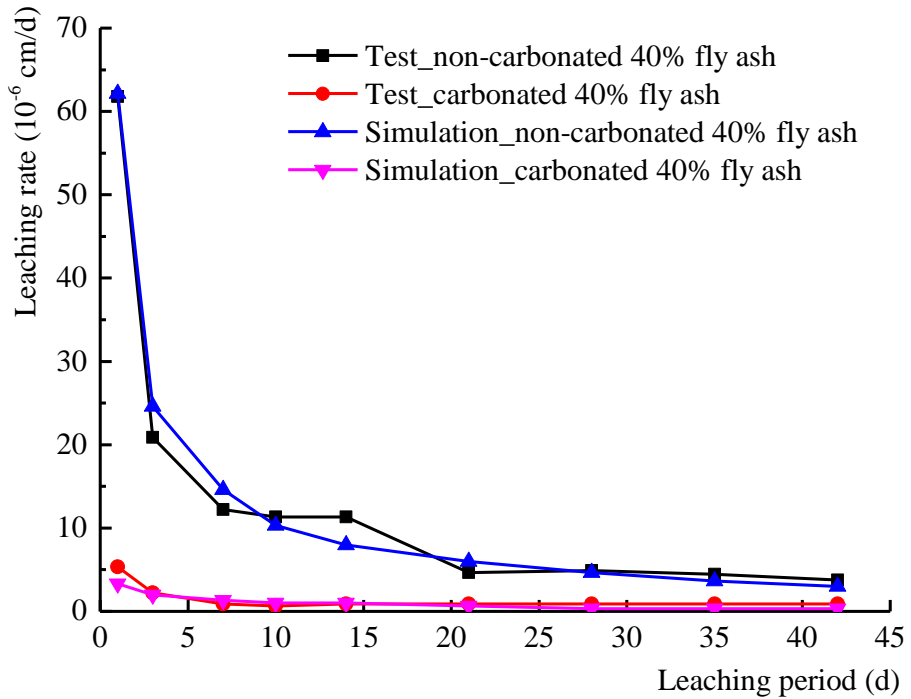
Fig. 7 Leaching rates of Cu in 40% cement-solidified fly ash



406

407

Fig. 8 Leaching rates of Cu in 60% cement-solidified fly ash



408

409

Fig. 9 Leaching rates of Pb in 40% cement-solidified fly ash

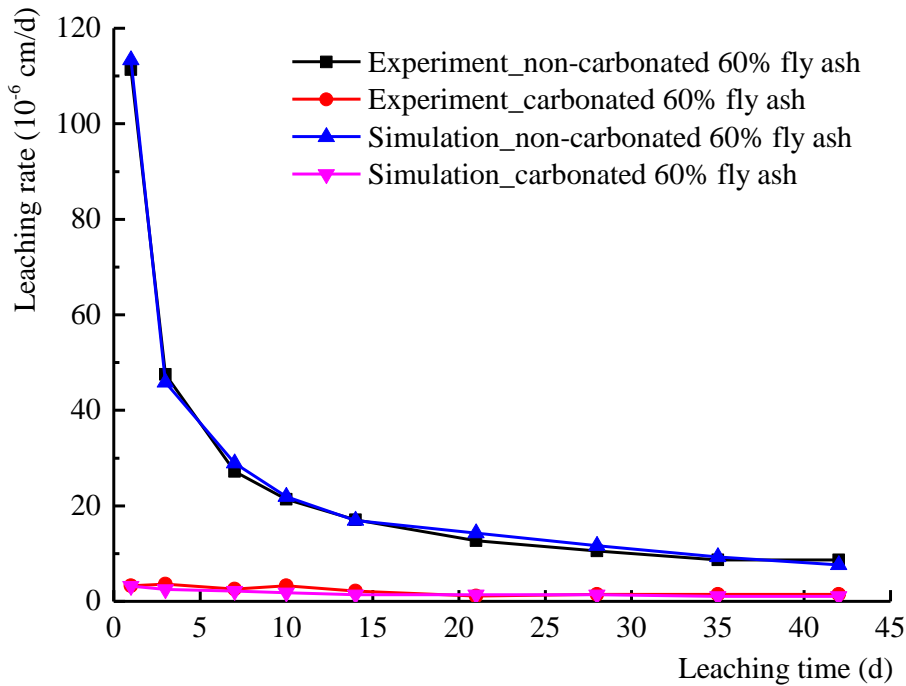


Fig. 10 Leaching rates of Pb in 60% cement-solidified fly ash

From Figs. 7-10, the simulated leaching rates of Pb agree well those measured in the leaching tests, while the agreement between the simulated and tested leaching rates of Cu are less satisfactory. This may be owing to that the calculation method of chemical activity factor for Cu (equation (15)) was not sufficiently accurate, which should include the impacts of not only the carbonation degree, but also the pH and ionic characteristics of the cement-based materials. Further research is required in this direction. Nevertheless, the modified model has correctly predicted the decrease of the leaching rate of Cu with increase of leaching time and the increase in leaching rate after the samples were carbonated (from the Figs. 7 and 8), which is consistent with the leaching tests results.

The leaching rate of Cu in carbonated cement-solidified fly ash is generally higher than that of the un-carbonated as shown in Figs. 7 and 8. The increased leaching of Cu from the cement-solidified samples is in line with the results of Valls and Vázquez [49] and Ginneken et al. [25], but in contrast with the results of Gerven et al. [18], which may be due to the use of different types of fly ash, leachant pH, mixing ratio [19] and leaching procedures [48]. Based on the experiments of this paper, it is clear that carbonation does not help in retaining Cu in the cement-

428 based materials. One of the reasons is that carbonation leads to a decrease in pH of the cement-
429 solidified fly ash (chemical retention), which deteriorates the chemical stability of Cu element
430 in the form of hydroxide or carbonate under high-pH conditions, and is beneficial to the
431 solubility of Cu element, thus increases the content of leachable Cu and its leaching rate [18].
432 The other is that though the calcium carbonate formed during the carbonation can block the
433 leaching of the heavy metals (physical retention) [23, 50], the micro-crack induced by the over-
434 carbonation can also promote leaching, and this may have occurred in this experiment.
435 In addition, there is little difference in the long-term leaching rates of Cu in 40% and 60%
436 cement-solidified fly ash, whether before or after carbonation. It can be seen from equation (17)
437 that the leaching rate of leaching elements is proportional to the ratio of the leaching amount
438 and the total amount of the leaching elements. In addition, for both Cu and Pb, Table 2 shows
439 that the total amount of them is in proportional to the fly ash ratio. Thus, for a given leaching
440 rate, the leaching amount of Cu varies linearly with fly ash ratio. A cement-solidified sample
441 with higher fly ash ratio will leach more Cu.

442
443 The leaching rate of Pb of the carbonated cement-solidified fly ash was obviously lower than
444 that of the un-carbonated (Figs. 9 and 10). The results agreed with those of Gerven et al. [18]
445 and Sanchez et al. [51], but disagreed with those of Shafique et al. [52]. It is noteworthy to
446 mention that the leaching in Shafique et al. [52] was mainly caused by micro-cracks after a
447 significant decrease in porosity caused by carbonation. Because of the formation of lead
448 carbonate (PbCO_3) from carbonation, Pb appears less solubility in neutral than high pH [18].
449 Hence, the leaching of Pb is influenced by both chemical and physical retentions. Considering
450 the majority of the published results on leaching of Pb and the observations from this paper, it
451 can be concluded that chemical retention has played a more important role than physical
452 retention in reducing Pb leaching. Contrast to a rather constant long-term leaching rate of Cu
453 for the samples with different fly ash ratios, the long-term leaching rate of Pb increases as the
454 fly ash ratio increases. Hence, an increase of fly ash ratio will result in leaching more Pb than
455 Cu, which can be accounted for that the amount of Pb is larger than that of Cu in fly ash (Table

456 2).

457

458 Overall, it can be concluded that the effect of carbonation on the leaching of heavy metals is

459 not always favorable.

460

461 **5. Conclusions**

462 An existing supercritical carbonation model has been modified to consider carbonation of

463 cement-solidified fly ash of various mixture ratios. This model was further combined with a

464 leaching model to simulate leaching of heavy metals, i.e., Cu and Pb, in cement-solidified fly

465 ash with and without being carbonated. Carbonation and leaching tests were carried out to

466 verify the new models. The effect of supercritical carbonation on the properties of the cement-

467 solidified fly ash were studied both numerically and experimentally. From the study the

468 following observations have been made:

469

470 (1) Using CO₂ absorption instead of calcium carbonate to measure carbonation degree is

471 more accurate in simulating carbonation process of cement-based materials with

472 various mixtures.

473

474 (2) The strength of cement-solidified fly ash after carbonation may be reduced, depending

475 on the carbonation duration and fly ash ratio.

476

477 (3) The leaching of Cu and Pb before and after carbonation have shown that carbonation

478 is not always beneficial to the retention of heavy metals, depending on the combined

479 effect of chemical and physical retentions.

480

481 (4) Leaching of Cu and Pb increases as fly ash ratio increases, while the increase in Pb

482 leaching is more substantial.

483

484 **Acknowledgements**

485 This study was funded by the National Nature Science foundation of China (grant numbers

486 51578181), Natural Science Foundation of Guangdong Province (grant numbers

487 2016A030313665) and Shenzhen Science and Technology Plan Project (grant numbers
488 JCYJ 20150327155221857). The authors would like to extend their appreciation to
489 Shenzhen Carbon Storage Cement-based Materials Engineering Laboratory. The authors
490 from Lancaster University are grateful for the support from H2020-MSCA ITN-SAFERUP
491 (grant number 765057).....

492

493 **Reference**

494 [1] C. Zhu, H. Tian, K. Cheng, K. Liu, K. Wang, S. Hua, J. Gao, J. Zhou, Potentials of whole
495 process control of heavy metals emissions from coal-fired power plants in China, *J. Clean*
496 *Prod.*, 114 (2016) 343-351.

497 [2] B. Prasad, K. Sangita, Heavy Metal Pollution Index of Ground Water of an Abandoned
498 Open Cast Mine Filled with Fly Ash: a Case Study, *Mine Water Environ.*, 27 (2008) 265-
499 267.

500 [3] S.A. Montzka, E.J. Dlugokencky, J.H. Butler, Non-CO₂ greenhouse gases and climate
501 change, *Nature*, 476 (2011) 43-50.

502 [4] J. Hays, Garbage and Recycling in China,
503 <http://factsanddetails.com/china/cat10/sub66/item1111.html>, 2014.

504 [5] J. Tang, M. Petranikova, C. Ekberg, B.-M. Steenari, Mixer-settler system for the recovery
505 of copper and zinc from MSWI fly ash leachates: An evaluation of a hydrometallurgical
506 process, *J. Clean Prod.*, 148 (2017) 595-605.

507 [6] L. Wang, Q. Chen, I.A. Jamro, R.D. Li, H.A. Baloch, Accelerated co-precipitation of lead,
508 zinc and copper by carbon dioxide bubbling in alkaline municipal solid waste incinerator
509 (MSWI) fly ash wash water, *RSC Adv.*, 6 (2016) 20173-20186.

510 [7] J.B.M. Dassekpo, X.X. Zha, J.P. Zhan, J.Q. Ning, The effects of the sequential addition
511 of synthesis parameters on the performance of alkali activated fly ash mortar, *Results in*
512 *Physics*, 7 (2017) 1506-1512.

513 [8] J.E. Aubert, B. Husson, N. Sarramone, Utilization of municipal solid waste incineration
514 (MSWI) fly ash in blended cement. Part 1: Processing and characterization of MSWI fly

- 515 ash, *J. Hazard. Mater.*, 136 (2006) 624-631.
- 516 [9] L. Cang, Y.J. Wang, D.M. Zhou, Y.H. Dong, Heavy metals pollution in poultry and
517 livestock feeds and manures under intensive farming in Jiangsu Province, China, *J.*
518 *Environ. Sci.*, 16 (2004) 371-374.
- 519 [10] E. Sakai, S. Miyahara, S. Ohsawa, S.H. Lee, M. Daimon, Hydration of fly ash cement,
520 *Cement Concrete Res*, 35 (2005) 1135-1140.
- 521 [11] L.H.J. Martin, F. Winnefeld, E. Tschopp, C.J. Muller, B. Lothenbach, Influence of fly ash
522 on the hydration of calcium sulfoaluminate cement, *Cement Concrete Res*, 95 (2017) 152-
523 163.
- 524 [12] J. Vargas, A. Halog, Effective carbon emission reductions from using upgraded fly ash in
525 the cement industry, *J. Clean Prod.*, 103 (2015) 948-959.
- 526 [13] T. Hemalatha, A. Ramaswamy, A review on fly ash characteristics - Towards promoting
527 high volume utilization in developing sustainable concrete, *J. Clean Prod.*, 147 (2017)
528 546-559.
- 529 [14] J.E. Aubert, B. Husson, A. Vaquier, Use of municipal solid waste incineration fly ash in
530 concrete, *Cement Concrete Res*, 34 (2004) 957-963.
- 531 [15] M. Arezoumandi, T.J. Looney, J.S. Volz, Effect of fly ash replacement level on the bond
532 strength of reinforcing steel in concrete beams, *J. Clean Prod.*, 87 (2015) 745-751.
- 533 [16] M. Arezoumandi, J.S. Volz, Effect of fly ash replacement level on the shear strength of
534 high-volume fly ash concrete beams, *J. Clean Prod.*, 59 (2013) 120-130.
- 535 [17] H.S. Shi, L.L. Kan, Leaching behavior of heavy metals from municipal solid wastes
536 incineration (MSWI) fly ash used in concrete, *J. Hazard. Mater.*, 164 (2009) 750-754.
- 537 [18] T. Van Gerven, D. Van Baelen, V. Dutré, C. Vandecasteele, Influence of carbonation and
538 carbonation methods on leaching of metals from mortars, *Cement Concrete Res*, 34 (2004)
539 149-156.
- 540 [19] Q.J. Yu, S. Nagataki, J.M. Lin, T. Saeki, M. Hisada, The leachability of heavy metals in
541 hardened fly ash cement and cement-solidified fly ash, *Cement Concrete Res*, 35 (2005)
542 1056-1063.

- 543 [20] M. Moranville, S. Kamali, E. Guillon, Physicochemical equilibria of cement-based
544 materials in aggressive environments - experiment and modeling, *Cement Concrete Res*,
545 34 (2004) 1569-1578.
- 546 [21] X.X. Zha, H.Y. Wang, P.Y. Xie, C. Wang, P. Dangla, J.Q. Ye, Leaching resistance of
547 hazardous waste cement solidification after accelerated carbonation, *Cem. Concr.*
548 *Compos.*, 72 (2016) 125-132.
- 549 [22] E.E. Berry, Fly Ash for Use in Concrete. Part 1, A Critical Review of the Chemical,
550 Physical and Pozzolanic Properties of Fly Ash, Energy, Mines and Resources Canada,
551 CANMET1976.
- 552 [23] A.V. Saetta, B.A. Schrefler, R.V. Vitaliani, The carbonation of concrete and the
553 mechanism of moisture, heat and carbon dioxide flow through porous materials, *Cement*
554 *Concrete Res*, 23 (1993) 761-772.
- 555 [24] P.J. Gunning, C.D. Hills, P.J. Carey, Accelerated carbonation treatment of industrial
556 wastes, *Waste Management*, 30 (2010) 1081-1090.
- 557 [25] L. Van Ginneken, V. Dutre, W. Adriansens, H. Weyten, Effect of liquid and supercritical
558 carbon dioxide treatments on the leaching performance of a cement-stabilised waste form,
559 *Journal of Supercritical Fluids*, 30 (2004) 175-188.
- 560 [26] J.Y. Shen, P. Dangla, M. Thiery, Reactive transport modeling of CO₂ through
561 cementitious materials under CO₂ geological storage conditions, *Int. J. Greenh. Gas*
562 *Control*, 18 (2013) 75-87.
- 563 [27] X.X. Zha, M. Yu, J.Q. Ye, G.L. Feng, Numerical modeling of supercritical carbonation
564 process in cement-based materials, *Cement Concrete Res*, 72 (2015) 10-20.
- 565 [28] Y. Li, The theoretical and experimental study of supercritical carbon dioxide on
566 transforming cement-base building materials, Harbin Institute of Technology, 2012.
- 567 [29] G. Feng, Experimental and numerical study of accelerated carbonation in cement brick
568 and tile, Harbin Institute of Technology, 2013.
- 569 [30] M.G. Richardson, Carbonation of reinforced concrete: its causes and management,
570 University College Dublin, 1988.

- 571 [31] V.G. Papadakis, C.G. Vayenas, M.N. Fardis, Fundamental modeling and experimental
572 investigation of concrete carbonation, *ACI Mater. J.*, 88 (1991) 363-373.
- 573 [32] Chemical reagent-Preparations of reagent solutions for use in test methods, GB/T 603-
574 2002.
- 575 [33] L. Chen, Research on concrete carbonation model and its parameters, Xi'an University of
576 Architecture and Technology, 2007.
- 577 [34] J.-B.M. Dassekpo, X. Zha, J. Zhan, J. Ning, The effects of the sequential addition of
578 synthesis parameters on the performance of alkali activated fly ash mortar, *Results in*
579 *Physics*, 7 (2017) 1506-1512.
- 580 [35] J.B.M. Dassekpo, J.Q. Ning, X.X. Zha, Potential solidification/stabilization of clay-waste
581 using green geopolymer remediation technologies, *Process Saf. Environ. Protect.*, 117
582 (2018) 684-693.
- 583 [36] I. Phummiphan, S. Horpibulsuk, R. Rachan, A. Arulrajah, S.-L. Shen, P. Chindaprasirt,
584 High calcium fly ash geopolymer stabilized lateritic soil and granulated blast furnace slag
585 blends as a pavement base material, *J. Hazard. Mater.*, 341 (2018) 257-267.
- 586 [37] W. Jie, J.B.M. Dassekpo, C.Y. Wan, X.X. Zha, Experimental and numerical modeling of
587 chloride diffusivity in hardened cement concrete considering the aggregate shapes and
588 exposure-duration effects, *Results in Physics*, 7 (2017) 1427-1432.
- 589 [38] J. Li, X. Zhao, Z. Liu, A new equation for calculating specific heat capacity of
590 supercritical fluid, *Proceedings of the 2009 Conference on Engineering*
591 *Thermodynamics and Energy Utilization Dalian*, 2009, pp. 1-6.
- 592 [39] L. Shi, X.F. Zhang, X.G. Zhang, B.X. Han, G.Y. Yang, H.K. Yan, Constant-Volume Heat
593 Capacity of Mixed Supercritical Fluids and Molecular Interaction in the Systems, *Chinese*
594 *Chemical Letters*, (1999) 873-874.
- 595 [40] S.J. Kwon, H.W. Song, Analysis of carbonation behavior in concrete using neural network
596 algorithm and carbonation modeling, *Cement Concrete Res*, 40 (2010) 119-127.
- 597 [41] N.R. Short, P. Purnell, C.L. Page, Preliminary investigations into the supercritical
598 carbonation of cement pastes, *Journal of Materials Science*, 36 (2001) 35-41.

- 599 [42] Y. Song, Y. Wang, P. Song, Q. Li, Nonequilibrium Thermodynamics Study of Nuclide
600 Migration Behavior in the Cement Based Radioactive Waste Forms, Journal of Henan
601 University(Natural Science), (2006) 21-24.
- 602 [43] Standard test method for leachability of low and intermediate level solidified radioactive
603 waste forms, GB/T 7023-2011.
- 604 [44] F.R. Wu, Y. Masuda, S. Nakamura, S. Sato, Influence of mixture proportion and curing
605 condition on contribution of fly ash to strength of concrete, in: N.Q. Feng, G.F. Peng (Eds.)
606 Environmental Ecology and Technology of Concrete, Trans Tech Publications Ltd,
607 Zurich-Uetikon, 2006, pp. 235-241.
- 608 [45] E. L. White, D. M. Roy, P. D. Cady, Modeling the Effects of Fly Ash Characteristics and
609 Mixture Proportions on Strength and Durability of Concretes, 1986.
- 610 [46] P. Chindapasirt, C. Jaturapitakkul, T. Sinsiri, Effect of fly ash fineness on compressive
611 strength and pore size of blended cement paste, Cem. Concr. Compos., 27 (2005) 425-
612 428.
- 613 [47] A. Neves Junior, R.D. Toledo Filho, E.d.M. Rego Fairbairn, J. Dweck, A study of the
614 carbonation profile of cement pastes by thermogravimetry and its effect on the
615 compressive strength, Journal of Thermal Analysis and Calorimetry, 116 (2014) 69-76.
- 616 [48] F. Lombardi, T. Mangialardi, L. Piga, P. Sirini, Mechanical and leaching properties of
617 cement solidified hospital solid waste incinerator fly ash, Waste Management, 18 (1998)
618 99-106.
- 619 [49] S. Valls, E. Vázquez, Accelerated carbonatation of sewage sludge – cement–sand mortars
620 and its environmental impact, Cement Concrete Res, 31 (2001) 1271-1276.
- 621 [50] P.J. Dewaele, E.J. Reardon, R. Dayal, Permeability and porosity changes associated with
622 cement grout carbonation, Cement Concrete Res, 21 (1991) 441-454.
- 623 [51] F. Sanchez, C. Gervais, A.C. Garrabrants, R. Barna, D.S. Kosson, Leaching of inorganic
624 contaminants from cement-based waste materials as a result of carbonation during
625 intermittent wetting, Waste Management, 22 (2002) 249-260.

626 [52] M.S.B. Shafique, J.C. Walton, N. Gutierrez, R.W. Smith, A.J. Tarquin, Influence of
627 carbonation on leaching of cementitious wasteforms, J. Environ. Eng.-ASCE, 124 (1998)
628 463-467.
629